RSC Advances

ROYAL SOCIETY OF CHEMISTRY

www.rsc.org/advances

RSC Adances

COMMUNICATION

A facile novel preparation of three-dimensional Ni@graphene by catalyzed glucose blowing for high-performance supercapacitor electrode

Received 00th January 20xx,
Accepted 00th January 20xx

DOI: 10.1039/x0xx00000x

www.rsc.org/advances

Lizhong Liu, huanli Wang, Zhengwei Zhou, Guangyu He, Xiaoqiang Sun, Qun Chen and Haiqun Chen*

Three-dimensional Ni@graphene (NG) was prepared for the first time at a low temperature by a one-step facile calcination method. The obtained NG showed a high specific capacitance of 765 F/g at a current density of 1 A/g and only 5% loss of the initial specific capacitance after 3000 charge/discharge cycles.

Three dimensional (3D) graphene has been widely applied in various fields, such as super capacitors, sensors, catalysis and energy storage, due to its ultrahigh conductivity, fast mass and electron transport kinetics, large specific surface area and unique graphene structure.[1-7] However, the preparation methods, such as chemical vapor deposition (CVD) and chemical exfoliation method,[1,3] remain relatively complex and difficult. Recently, Wang et al.[8] prepared 3D strutted graphene through a simple high-temperature calcination method with glucose or sucrose as raw material. The obtained graphene not only retained the robust structural integrity, but also possessed high electrical conductivity, surface area, mechanical strength and elasticity due to their topological structure, which led to better electrochemical properties than two dimensional graphene. Nevertheless, this preparation process requires a high temperature (1350 °C) and high-quality devices, which will restrict its further applications.

Herein, we developed a facile and scalable in situ synthetic strategy to construct a 3D nickel skeleton-supported graphene composite, which was designated as NG [see the Electronic Supplementary Information (ESI) for more experimental details]. The possible synthetic route of NG was surmised and illustrated in Fig. 1. The in situ formation of nickel skeleton and the growth of the outer 3D graphene were accomplished simutaneously in one calcination process. During the calcination process (Fig. S1), glucose which was utilized as carbon source was gradually polymerized to form glucose-derived polymers; NH_4Cl and $NiCl_2{\cdot}6H_2O$ were homogeneously dispersed and adsorbed in the glucose-derived polymers. Then HCl and NH_3 gases were released slowly from the decomposition of NH_4Cl, resulting in cavities inside the glucose-derived polymers. With continuous heating, HCl and NH_3 generated in the system expanded, walls of the cavities became thinner and thinner. Subsequently, Ni^{2+} was reduced to form metal Ni skeleton, which acted not only as a catalyst to promote the graphitization of the carbon source from glucose to few-layer graphene, but also as a frame to support the 3D nanostructure. Delightedly, with Ni as catalyst, the carbonization temperature was greatly reduced to temperature of 900 °C, which was relatively low compared with 1350°C reported by other groups.[8] Moreover, the as-prepared NG exhibited high specific capacitance with great stability, which is better than not only that of Ni–RGO[9] and Ni@C[10] composites, but also that of $NiCo_2O_4$–RGO[11] and Co_3O_4–RGO[12] composites we prepared previously. For comparison, the metal-catalyst-free sample (denoted as MCF) was prepared without adding $NiCl_2{\cdot}6H_2O$ and the blowing-reagent-free sample (denoted as BRF) was prepared without adding NH_4Cl [see the ESI for more experimental details].

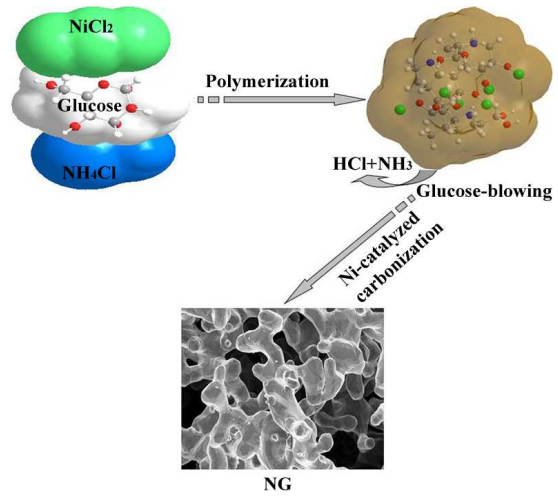

Fig. 1. Schematic illustration of NG fabrication.

Key Laboatory of Advanced Catalytic Materials and Technology,.Changzhou University, Jiangsu Province, Changzhou 213164, China.
E-mail: hqchenyf@hotmail.com(H Chen).
Tel: +86 519 86330088; Fax: +86 519 86330086
Electronic Supplementary Information (ESI) available: [details of any supplementary information available should be included here].

Besides, the obtained NG and BRF samples were etched by 3 M HCl and denoted as E-NG and E-BRF, respectively.

The morphology of NG was observed through TEM and FESEM. As shown in Fig. 2a, during the calcination process, Ni^{2+} was reduced to nickel skeleton with different morphologies. The skeleton was enfolded with few-layered graphene converted from glucose-derived polymers, which was similar to nickel skeleton-containing 3D graphene prepared by CVD methods.[13] The TEM images of NG (Fig. 2b) are also consistent with the above description. From the HRTEM images of the edge of NG (Fig. 2c and d), the lattice fringes of Ni with the d-spacing of 0.21 nm and few-layered graphene were observed.[14] However, the TEM image of the E-NG (Fig. 2e) shows that only small amount of metal Ni nanoparticles were left after the etching process and rapped with silk veil-like graphene sheets, showing that the thin graphene layer collapsed due to its low mechanical stability.[15] On the other hand, the graphene structure was not observed in BRF or MCF (Fig. 2f) when either $NiCl_2 \cdot 6H_2O$ or NH_4Cl was absent, which shows that both $NiCl_2 \cdot 6H_2O$ and NH_4Cl are essential to the formation of 3D interconnected Ni@graphene structure. Moreover, sufficient amount of $NHCl_4$ is needed for the successful preparation of the 3D Ni@graphene composite (Fig. S2). The possible reason is that due to the thermal expansion of the chemically released gases from NH_4Cl in the system, the cavities generated in the glucose-derived polymers grew sufficiently to make the walls of the cavities become thin enough, which facilitated the dispersion of metal Ni in the glucose-derivative and increased the specific surface areas of carbon source as well as the finally formed metal Ni. After the formation of Ni skeleton, the carbon atoms dissolved into the metal Ni at high temperature.[16] During the subsequent cool-down, the dissolved carbon atoms precipitated on the surface of the Ni skeleton to form uniform few-layered graphene membranes,[17] thus 3D Ni@graphene composite was obtained. However, when the amount of NH_4Cl was inadequate, the specific surface areas of metal Ni and the glucose-derivative relatively decreased, which restricted the metal Ni catalyzed graphitization reaction for carbon source.

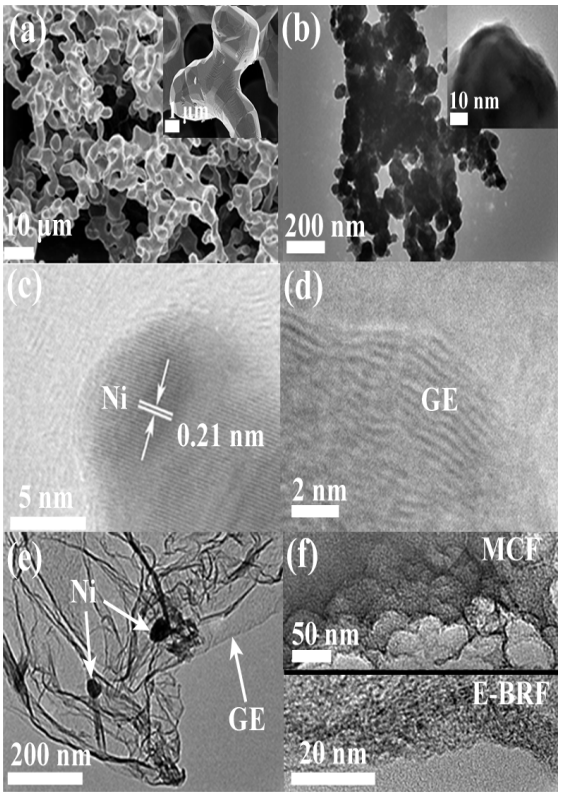

Fig. 2. Typical FESEM images of NG (a); TEM images of NG (b), E-NG (e), MCF and E-BRF (f); HRTEM images of NG taken near the edges of the sample (c, d and the inset of b).

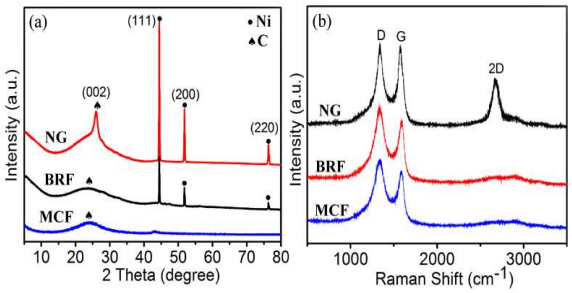

Fig. 3. (a) XRD patterns and (b) Raman spectra of NG, BRF and MCF.

The X-ray diffraction (XRD) patterns of the as-prepared NG, BRF and MCF are shown in Fig. 3a. Compared with those of BRF and MCF, the XRD patterns of NG shows a relatively strong and sharp characteristic (002) peak of graphite at 2θ = 26.0°, suggesting that the graphitization degree of the carbon source increased when both NH_4Cl and $NiCl_2 \cdot 6H_2O$ were employed. Meanwhile, the XRD pattern of NG and BRF present additional diffraction peaks at 2θ = 44.5, 51.8, and 76.4°, which can be indexed to the (111), (200) and (220) planes of cubic Ni (JCPDS: 04-0850), indicating that Ni^{2+} ion was converted into metallic Ni after being calcinated at 900 °C. Nevertheless, the XRD patterns in Fig. S3 showed that the graphitization degree of the samples calcinated respectively at 600, 700, 800, and 850 °C is not high enough to obtain 3D Ni@graphene composite.

Compared with the Raman spectrum of MCF and BRF (Fig. 3b), a narrow 2D peak appeared in the Raman spectrum of the obtained NG at 2700 cm^{-1} with a full width at a half maximum of 70 cm^{-1}, which features a well-graphitized few-layered graphene.[8,18] Moreover, the D/G intensity ratio of NG decreased compared with that of MCF and BRF, which suggests the decrease of the material defect, namely the increase of the sp^2 hybridized carbon domain. The XRD and Raman results are in accordance with that of TEM, indicating the transformation of glucose to graphene was due to the synergistic effect of catalysis of in-situ generated Ni and the thermal decomposition of NH_4Cl.

N_2 adsorption-desorption isotherms were applied to investigate the porous structure and surface area of the NG composite. As shown in Fig. S4, the N_2 isotherm of the NG composite is close to Type IV, revealing the existence of mesopores. The measurements indicated that the sample has a Brunauer-Emmett-Teller (BET, nitrogen, 77 K) surface area of 99.86 m^3/g with a Barrett-Joyner-Halenda (BJH) desorption average pore diameter of 4.06 nm. In addition, the ICP-AES test result showed that the content of Ni out of 10 mg of NG was 5.662 mg. It means the graphene content of NG is about 43.38%, which is consistent with TG results (Fig. S5).

Electrochemical measurements were conducted to evaluate the potential application prospect of NG as electrodes for supercapacitors. Representative CV curves of NG and bare Ni film electrodes at a scan rate of 10 mV/s are shown in Fig. 4a. The shape of the CV curves reveals the pseudocapacitive characteristics with a pair of redox peaks in the potential range from -0.1 to 0.6 V, which is mainly attributed to the faradic reaction related to Ni^{2+}/Ni^{3+}.[19,20] Compared with bare Ni film, the higher peak current density of NG is an indication of better charge transfer due to 3D graphene's good electrical conductivity.

Fig. 4b-c display the galvanostatic discharge testing results for NG and bare Ni film, respectively. The nonlinear discharge curves further verify the pseudo-capacitance behavior of NG.[21,22] The specific capacitance (C_m) was calculated according to the following equation:

$$C_m = \frac{I \times t}{m \times \Delta V} \text{ (F/g)}$$

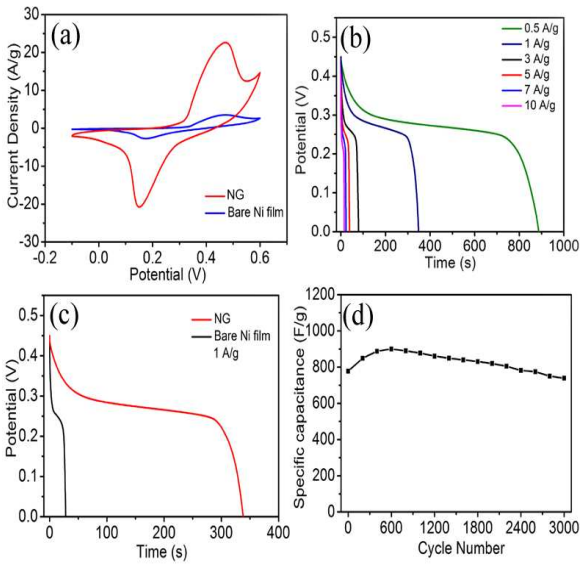

Fig. 4. (a) CV curves of NG and bare Ni film acquired at a scan rate of 10 mV/s; (b) galvanostatic discharge curves of NG; (c) galvanostatic charge-discharge curves of NG and bare Ni film; (d) stability test for NG at 1 A/g.

where I, t, ΔV and m is the discharge current (A), time (s), potential drop (V), and the mass of active material on working electrode (g), respectively.

The C_m reached 986 F/g at a low current density of 0.5 A/g, which remained at 444 F/g at a higher current density of 10 A/g. Meanwhile, the capacitance of bare Ni film is only 95 F/g at 1 A/g, which is much lower than 778 F/g for NG (Fig. 3c). It demonstrates that 3D graphene structure helps to improve the capacity of the interfacial energy storage. Besides, the C_m of NG is higher than that of porous Ni (416.6 F/g, 1A/g),[22] Ni-RGO (547.3 F/g, 1A/g),[9] Ni@C (530 F/g, 1A/g),[10] NiO/C (356.2 F/g, 1 A/g),[23] NiO/FCNTs (526 F/g, 1 A/g),[24] $NiCo_2O_4$-RGO (737 F/g, 1 A/g),[11] indicating the NG composite has an excellent supercapacitive performance.

The cycling stability of the NG electrode at 1 A/g is shown in Fig. 4d. The C_m presented an obvious increase and reached a maximum value of 900 F/g after 600 cycles, indicating metal Ni gradually undergoes an electrochemical oxidation into NiO during the charge and discharge cycling.[9,20] After 3000 cycles, 95% of the initial C_m remained, showing good cycling stability.

In conclusion, 3D Ni@graphene was synthesized through a simple and effective calcination method in one step. The calcination temperature of glucose graphitization was effectively decreased due to the catalysis of in-situ generated metal Ni. NG showed high C_m (765 F/g) and excellent cycle life in 2 M KOH at 1 A/g, which makes it a promising electrode for supercapacitors.

Acknowledgements

The financial supports from the National Natural Science Foundation of China (No. 51202020, 51472035), the Science and Technology Department of Jiangsu Province (BY2013024-04, BE2014089, BY2015027-18), Jiangsu Key Laboratory of Advanced Catalytic Materials and Technology (BM2012110, ZMF14020036) and the PAPD of Jiangsu Higher Education Institutions are gratefully acknowledged.

Notes and references

1 Z. Chen, W. Ren, L. Gao, B. Liu, S. Pei and H.M. Cheng. Nat. Mater., 2011, **10**, 424-428.
2 J. Yuan, J. Zhu, H. Bi, X. Meng, S. Liang, L. Zhang and X. Wang. Phys. Chem. Chem. Phys., 2013, **15**, 12940-12945.
3 K. Sheng, Y. Sun, C. Li, W. Yuan and G. Shi. Sci. Rep-UK., 2012, **2**, 1-5.
4 L. Zhang and G. Shi. J. Phys. Chem. C, 2011, **115**, 17206-1721.
5 F. Yavari, Z. Chen, A. V. Thomas, W. Ren, H. M. Cheng and N. Koratkara. Sci. Rep-UK, 2011, **1**, 1-5.
6 G. Srinivas, J. W. Burress, J. Fordab and T. Yildirim. J. Mater. Chem., 2011, **21**, 11323-11329.
7 G. K. Dimitrakakis, E. Tylianakis and G. E. Froudakis. Nano Lett., 2008, **8**, 3166-3170.

8 X. Wang, Y. Zhang, C. Zhi, X. Wang, D. Tang, Y. Xu, Q. Weng, X. Jiang, M. Mitome1, D. Golberg and Y. Bando. Nat. Commun., 2013, **4**, 1-8.
9 L. Niu, J. Wang, W. Hong, J. Sun, Z. Fan, X. Ye, H. Wang and S. Yang. Electrochim. Acta, 2014, **123**, 560-568.
10 L. Niu, Z. Li, J. Sun, Z. Fan, Y. Xu, P. Gong, S. Yang and J. Wang. J. Alloy. Compd., 2013, **575**, 152-157.
11 G. He, L. Wang, H. Chen, X. Sun and X. Wang. Mater. Lett., 2013, **98**, 164-167.
12 G. He, J. Li, H. Chen, J. Shi, X. Sun, S. Chen and X. Wang. Mater. Lett., 2012, **82**, 61-63.
13 A. C. Ferrari, J. C. Meyer, V. Scardaci, C. Casiraghi, M. Lazzeri, F. Mauri, S. Piscanec, Jiang, K. S. Novoselov, S. Roth and A. K. Geim. Phys. Rev. Lett., 2006, **97**, 187401-187404.
14 W. Li, S. Gao, L. Wu, S. Qiu, Y. Guo, X. Geng, M. Chen, S. Liao, C. Zhu, Y. Gong, M. Long, J. Xu, X. Wei, M. Sun and L. Liu. Sci. Rep-UK, 2013, **3**, 1-6.
15 J. S. Lee, S. I. Kim, J. C. Yoon and J. H. Jang. ACS Nano, 2013, **7**, 6047-6055.
16 X. Li, W. Cai, L. Colombo and R. S. Ruoff. Nano Lett, 2009, **9**, 4268-4272.
17 J. A. Rodríguez-Manzo, C. Pham-Huu and F. Banhart. ACS Nano, 2011, **5**, 1529-1534.
18 S. M. Yoon, W. M. Choi, H. Baik, H. J.Shin, I. Song, M. S. Kwon, J. J. Bae, H. Kim, Y. H. Lee and J. Y. Choi. ACS Nano, 2012, **6**, 6803-6811.
19 M. Alsabet and M. Grdeń. Electrocatalysis, 2015, **6**, 60-71
20 J. Zhu, S Chen, H Zhou and X. Wang. Nano Res., 2012, **5**, 11-18.
21 X. Wu, W. Xing, L. Zhang, S. Zhuo, J. Zhou and G. Wang. Powder Technol., 2012, **224**, 162-167.
22 H. Jiang, T. Sun, C. Li and Jan. Ma. RSC Adv., 2011, **1**, 954-957.
23 X. Wang, X. Wang, L. Yi, L. Liu, Y. Dai and H. Wu. J. Power Sources, 2013, **224**, 317-323.
24 C. Yuan, S. Xiong, X. Zhang, L. Shen, F. Zhang, B. Gao and L. Su. Nano Res., 2009, **2**, 722-732.